Earth Systems and Environment
https://doi.org/10.1007/s41748-026-01061-2

ORIGINAL ARTICLE

Wind Flow Analysis Beyond Orographic Effects: A Direction Turning-Gradient Approach for Urban Impact Quantification in Germany

Isidro A. Pérez[1] · **Mª Ángeles García**[1] · **Orelvis Valdés**[1]

Received: 19 November 2025 / Revised: 14 January 2026 / Accepted: 28 January 2026

Abstract

Wind direction is a variable that plays a secondary role in wind analyses since air flow is first studied. This paper focuses on its behaviour in ten cities and at two rural sites to investigate urban impact on wind direction. The database covered 18 years with a resolution of 1 km^2, and hourly values were used. Two main procedures were followed. The first calculated the wind rose with high angular resolution from the average wind in each region studied as opposed to the usual calculations, where wind direction is measured at only one site. Two smoothing procedures were posited to acquire information about the data structure and specific details in one-degree roses. Bandwidth selection was based on the agreement with observations. Results revealed that westerly directions prevailed, although three patterns were observed. The most frequent was formed by a wide westerly sector, which may be attributed to synoptic flow, followed by wind roses with well-determined directions, such as Munich, where a mixture of relief and synoptic pattern could explain the rose shape. Finally, orographic influence is noticeable in specific roses, such as in Cologne, where the Rhine valley influence prevails. The second procedure is based on the direction turning field followed by the gradient calculation. This analysis was performed following wind direction, and two noticeable patterns of clear turning changes were occasionally found. The first pattern was formed by very close turning centres, which appear to be linked to the city, such as in Frankfurt for the easterly flow with a turning of around 65 degrees. Stuttgart, where the direction rose was barely affected by orographic features, showed a similar value of direction turning for the southerly flow, although following a different pattern formed by turning bands. Robust statistics showed the urban-rural contrast. Finally, three groups may be formed following the response against the turning field, with the weakest being for the largest cities –Berlin and Hamburg– where pollutant dispersion could prevail. An intermediate response was observed for most of the studied sites. However, Stuttgart and Frankfurt stood out due to their accused turnings that might determine complex pollution transport.

✉ Isidro A. Pérez
isidro.perez@uva.es

[1] Department of Applied Physics, Faculty of Sciences, University of Valladolid, Paseo de Belén, 7, Valladolid 47011, Spain

Published online: 17 February 2026

Graphical Abstract

This paper investigates the urban influence of wind direction in Germany. Meteorological hourly values were downloaded from doi:https://doi.org/10.5676/DWD_CDC/TRY_Basis_v001 with a resolution of 1 km^2 and for a period of 18 years. Ten cities were selected following population size. Two rural sites were also considered. Wind direction analysis started with 1-degree roses that were smoothed with non-parametric regression. Three types were observed. The first group comprises roses strongly affected by orographic impact, such as in Düsseldorf. Hamburg represents the second type, which is featured by a wide west sector where the synoptic pattern prevails. Finally, the Munich rose is an example of sites where wind directions are well defined. A second analysis involved direction turning. In this case, average wind velocity was calculated in every region (represented by the black arrow). Wind direction turning was then obtained and was positive for anticyclonic turnings (in red) and negative for cyclonic turnings (in blue). Turning isolines were plotted following 16 wind sectors given by the average wind direction. Under specific flows, turning centres linked to cities appeared. In these cases, the average gradient was low due to opposite directions in the region, although the average of gradient magnitudes may be noticeable. Two representative situations are presented. Turning centres were well defined in Frankfurt under east flow where marked anticyclonic turning was noticeable in a transect from SE to NW. However, turning bands were noted in Stuttgart under south flow, with cyclonic turning in a transect from south to north. This research thus evidences the orographic influence and relevant wind patterns that impact pollution transport, where marked turnings are observed, whereas dispersion prevailed when direction turnings are less defined.

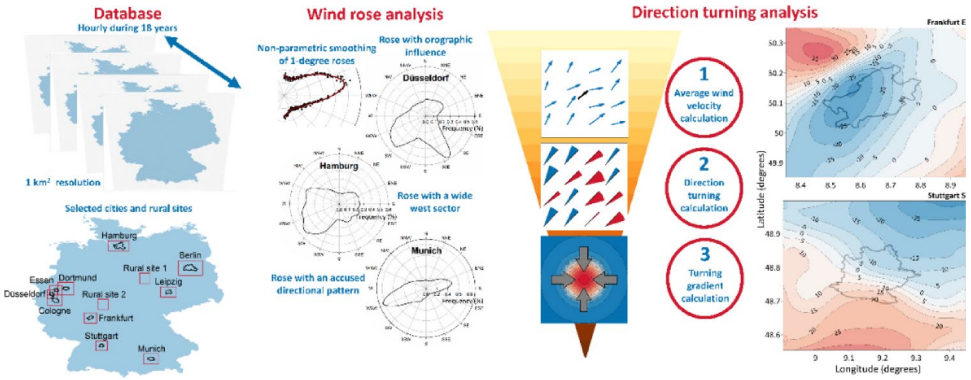

Highlights

- Three types of direction roses were obtained; two were mainly linked with the circulation pattern and the third with orography.
- Turning field shape was investigated with gradient calculations.
- Two turning schemes of wind direction were observed, with turning centres in Frankfurt and turning bands in Stuttgart standing out.
- Marked average gradients were linked with synoptic flow, whereas opposite gradients around the city revealed urban influence.
- Hamburg and Berlin stood out for having the lowest urban influence.

Keywords Wind rose · Direction field · Mesoscale · Urban ventilation

1 Introduction

Cities are spaces with features that differ when compared to those of natural sites. Effects such as the urban island in temperature or air pollution have been investigated to suggest solutions for the problems observed in certain cities. As regards the urban heat island, the rising warm air over the urban core forces the surface-level inflow of cooler air of rural surroundings, as simulated by Brandi et al. (2024) who studied the wind field in Phoenix, Arizona. Moreover, this circulation is affected by orographic features, which determine direction changes in the city and the surrounding region.

This paper focuses on wind direction –a variable that has scarcely been investigated to date. The absence of any such analyses is due to the lack of information concerning this variable, since only a small number of databases include it. Moreover, changes in wind direction occur more quickly

than in other variables, such as temperature; hence its noise may obscure its patterns.

Most wind direction analyses are related to air pollution, such as Zhang et al. (2025a), who investigated ozone transport over Beijing. In contrast to these papers, the current study analyses wind direction over urban environments. To achieve this objective, a gridded database with sufficient spatial and temporal resolution was used.

Wind direction analysis may be considered the first step for wind flow analysis, which may be presented under various forms. One of these analyses is air parcel trajectory calculation. Although these trajectories may be used to investigate long-range transport of air pollutants, local trajectories may help in new building designs (Pardo-del Viejo and Fernández-Rodríguez 2025).

Another way to research wind direction considers the relationship between synoptic and local scales. Hwang et al. (2024) found no significant impact of local conditions against the synoptic scale in their analysis of $PM_{2.5}$ in South Korea. However, O_3 concentration did not depend on long-range transport in summer due to its short photochemical lifetime.

The current research considers two kinds of analyses for ten German cities and their surroundings together with two rural sites. Spatial extension falls into the mesoscale range, which comprises areas where orographic features impact air circulation –although overlapping with the synoptic pattern– with some microscale processes also being observed.

The first analysis involves the wind direction rose. Sen and Roesler (2020) presented the wind direction rose for Chicago, United States, with eight sectors where large and small frequencies are interspersed. When only two sites are available, a comparative study of wind direction for an urban and a rural site is possible, with one example being that presented by Garvey et al. (2009). Local conditions may be investigated with multiple roses inside the city, such as Ali-Taleshi et al. (2025), who studied local $PM_{2.5}$ sources with 15 polar plots in Tehran, Iran. Liu et al. (2025a) presented six wind direction roses in Nanjing, China, where directions were divided between daytime and night-time. Two of these stations were located inside the city and provided contrasting results, probably due to the meandering wind flow in this urban environment.

Prevailing wind directions are used to determine urban ventilation corridors, with planning for such urban ventilation corridors having originated in Germany (Li et al. 2023; Zhan et al. 2020). These corridors include three control zones: the action space (where air and thermal pollutions should be controlled), the compensation space (which are sources of fresh air), and air guidance channels (which link the action and compensation areas). Bing et al. (2021) suggested Sttutgart, Germany, as a model of urban ventilation corridor research and application.

Du et al. (2023) indicated that published studies that address ventilation corridors should consider the urban morphology, wind speed, or air paths. They suggested four basic criteria, with the first being that continuous air paths should be generated, i.e., the airflow should penetrate the urban frame. Moreover, wind speed should be high in urban ventilation corridors to ensure noticeable ventilation potential. Since corridor dimensions should guarantee sufficient ventilation, they considered not less than 45 m. Finally, corridor effectiveness should be satisfactory in the prevailing wind directions. They indicated that angles between corridors and wind directions should be less than 40° for a continuous air path. Yin et al. (2025) indicated that urban ventilation conditions improve not only when the open space and the mean building height increase but also when the open space road sinuosity decreases. These ventilation conditions are related with the wind direction in the city.

However, ventilation corridors –which are proposed to improve urban air quality and to reduce heat island problems– may have the opposite effect. For example, Han et al. (2022) observed that particulate matter concentrations were higher in four compensation spaces than those in the Xi'an central urban area, China. Injecting this cold air in the city centre might trigger pollution problems. Consequently, the cleanliness of ventilation corridors should be assessed so as to avoid any increase in air pollution in central urban areas.

The second analysis studies the spatial distribution of wind direction. Analyses usually employed to describe such a variable consider varied roses along the region investigated. For instance, Ketterer and Matzarakis (2014) presented five roses in Stuttgart that covered rural, suburban, urban and city centre environments. Mikhailuta et al. (2017) presented eight roses in Krasnoyarsk, in south-central Russia. Ng et al. (2011) divided Hong Kong, China, into 26 blocks and presented the wind rose for each block. In general, studies in which wind direction is isolated are scarce. Ashrafi et al. (2022) not only investigated the wind field for an urban lake under varied wind sectors but also presented isolated wind direction values. McQuillan et al. (2025) presented a wind direction analysed from satellite data focusing on the western portion of Lake Ontario, which showed noticeable wind streaks along the western shore. Wind fields are a frequent representation of wind flow over a region. In this case, wind direction information is indirect, and precise values depend on field resolution. Dou et al. (2024) considered Beijing, China, although the region studied was wide enough to mask wind changes at smaller scales. May et al. (2024) considered a higher resolution for Heidelberg, Germany, where mountains in the east determine a mountain-valley circulation pattern. Finally, Ebert and Weiss (2024)

investigated the wind field in a small region of only 1 km^2 in Berlin, Germany, where street channelling was the departure point for their analysis.

The current research considers a section where the selected cities are introduced and the database is described, followed by the description of the rose calculation and spatial analysis. The following section is devoted to results of wind roses in the twelve selected regions and the calculation of direction turning in these regions. A comparison to previous studies is presented in the discussion section.

2 Materials and Methods

2.1 Database

Ten cities were selected following their population and are presented in Fig. 1 together with their surrounding regions chosen for the analysis. Regions overlap in four of them (Cologne, Dortmund, Düsseldorf, and Essen) since they are very close. Moreover, two rural sites have been included where cities are not present. Rural site 1 lies approximately 100 km NW of Leipzig with some hills to the south, and Rural site 2 lies some 80 km NE of Frankfurt.

The database used is described by Krähenmann et al. (2018) and considers monthly, daily and hourly grids for 12 meteorological variables over the period 1995–2012 and with a spatial resolution of 1 km^2 that limits the analysis to large cities. This study mainly considers hourly values of the 10 m wind direction, although wind speed is sometimes employed in specific calculations, such as when determining average direction.

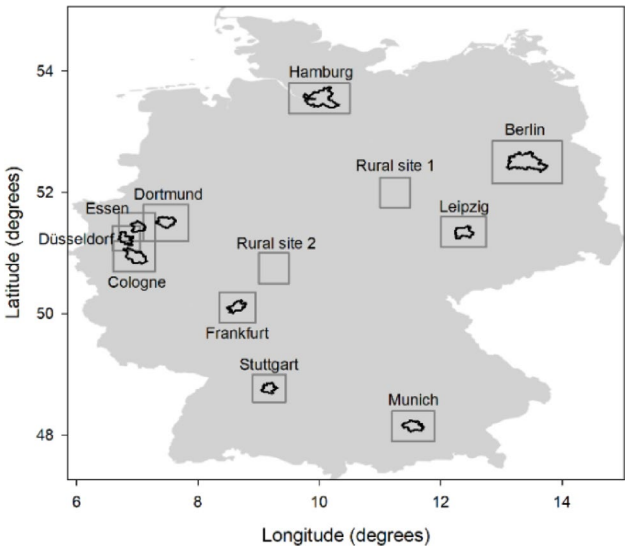

Fig. 1 - Selected cities and their regions chosen for the analysis

2.2 Calculation of Wind Direction and Speed Roses

The average wind vector was calculated with all the data for every region each hour. These hourly wind vectors were used to calculate detailed wind direction and speed roses with a 1-degree interval. The number of available observations allows this calculation. The main advantage of these roses is the satisfactory definition of narrow sectors. However, the observed scatter may be avoided by using certain smoothing procedures that retain the data trend, with two procedures being followed with the wind direction rose. The first was the kernel density calculation made in Matlab. Smoothing fundamentals can be seen in Fisher (1993) and Wilks (2019). A normal distribution was used, with an iterative procedure being considered to select bandwidth. Values in 1-degree steps were suggested for the bandwidth and the comparison between the experimental direction wind rose and each smoothed rose was made. This difference was seen to increase with bandwidth. First and second iterations were discarded due to their unsteady comparison values. However, a bandwidth of three degrees was selected since, from this bandwidth, the increase in the difference of experimental-smoothed values for two consecutive bandwidths seemed steadier than with the previous bandwidths. Moreover, a second smoothing was considered with a moving mean. In this case, varied windows in 1-degree steps were tested and the rose obtained with each window was compared with the previous one. Similar results to the previous procedure were obtained with a bandwidth of five degrees. This procedure was used for wind speed rose calculation, and the bandwidth was the same as for wind direction. The same bandwidth was used for all the cities analysed in this approach.

2.3 Spatial Analysis

Once the study region is established around each selected city, the average wind vector is calculated each hour. The direction of this average vector determines the sector in a 16-sector rose. The turned angle against the mean direction is calculated in each grid node. Positive values correspond to clockwise turnings and negative values to counter-clockwise turnings. The direction-turning interval extends from −180 to 180, and there are few extreme values. Once all the hourly values are calculated for each wind sector, they are averaged for all the studied period and Surfer isolines are presented. These isolines represent the wind turning in the selected region.

To investigate whether any noticeable changes are observed in the studied regions, turning gradients were calculated, and these indicate the peaks or valleys for contour lines of the direction turnings. These gradient calculations

were obtained with a secondary grid made with Surfer. The main advantage of this secondary grid is its orientation following latitude and longitude axes. The average of the gradient magnitudes was then obtained and compared with the magnitude of the average gradient vector. Three extreme possibilities presented in Fig. 2 were considered. Figure 2a presents a case where gradients of direction turnings –represented by isolines– have the same direction. In this situation, the magnitude of the average gradient –represented by a grey arrow– is comparable to the average of the gradient magnitudes calculated in each grid node. In Fig. 2b, a centre is visible that determines radial gradients. In this case, the average gradient is null, although the average of the gradient magnitudes is not. Figure 2c is similar to Fig. 2b, although a band rather than a centre is seen. Due to the limited extension of the regions studied, this case can sometimes be seen with small gradients.

3 Results

Two subsections are considered. The first studies the wind roses for mean wind in the investigated regions, while the second subsection examines the direction turning against the mean direction.

3.1 Wind Roses

Figure 3 presents the wind direction and speed roses. One common feature is that frequencies are low for directions from NW to N and from E to S, except for Cologne, Düsseldorf, and Essen. Moreover, frequencies from around SW were higher than frequencies from around NE.

Three rose groups may be seen. The first is formed by roses where directions are quite clearly defined, especially in Munich, but also in Dortmund, Frankfurt, and Rural site 2. Winds with an easterly component are clearly visible for Dortmund, since the highest frequencies are found in the ENE direction, whereas winds with the westerly component prevailed, although the highest frequencies were not so defined, since they are located in an interval from SW to WSW. The Frankfurt rose presents two opposite sectors where the highest frequencies were not as marked as for the Munich rose. Similar behaviour may be seen for Rural site 2.

The second group considers cities where a wide sector of frequent directions is visible, such as in Berlin, Hamburg, Leipzig, Stuttgart, and Rural site 1. Roses for Hamburg, Stuttgart and Rural site 1 presented a similar shape since similar frequencies are distributed in a wide west sector, with the highest frequency barley standing out in this sector. Roses for Berlin and Leipzig also present a wide sector of high frequencies, although one direction stands out vis-à-vis the rest. Frequencies are equally distributed in Hamburg and Rural site 1 for the low-frequency sector, whereas one frequency stands out for Berlin, Leipzig, and Stuttgart in this low-frequency sector.

Finally, the third group is formed by three cities where a narrow sector figures prominently, such as in Cologne, Düsseldorf, and Essen. These cities are quite close to one another and are influenced by the Rhine Valley. This sector stands out in Cologne, since frequencies are equally distributed outside it. The influence of this sector is also noticeable in Düsseldorf and is lower in Essen, since two additional opposite directions play a relevant role.

The impact of orographic influence can be seen with the roses from Cologne, Dortmund, Düsseldorf, and Essen. As Fig. 1 shows, these cities are quite close to one another. However, the greatest valley influence was observed in Cologne, where the most relevant feature is the high frequencies around the SE sector. This influence is not so relevant in Düsseldorf. A slight turning is evident, and perpendicular directions also figure prominently. However, the prevailing direction in Essen is the SW, with the influence of the valley playing a secondary role. Finally, this valley influence is missing in Dortmund.

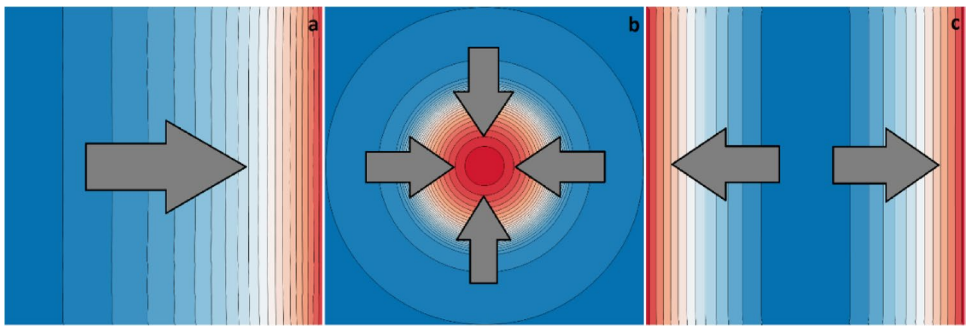

Fig. 2 - Examples of extreme gradients where isolines of direction turnings are presented and where grey arrows indicate the gradient where the arrow is located. **a**) An average gradient different from zero is represented by the grey arrow, **b**) a null average gradient, although a convergence centre for radial gradients can be seen, and **c**) a null average gradient, although two opposites gradients can be seen, since a centre for radial gradients does not appear

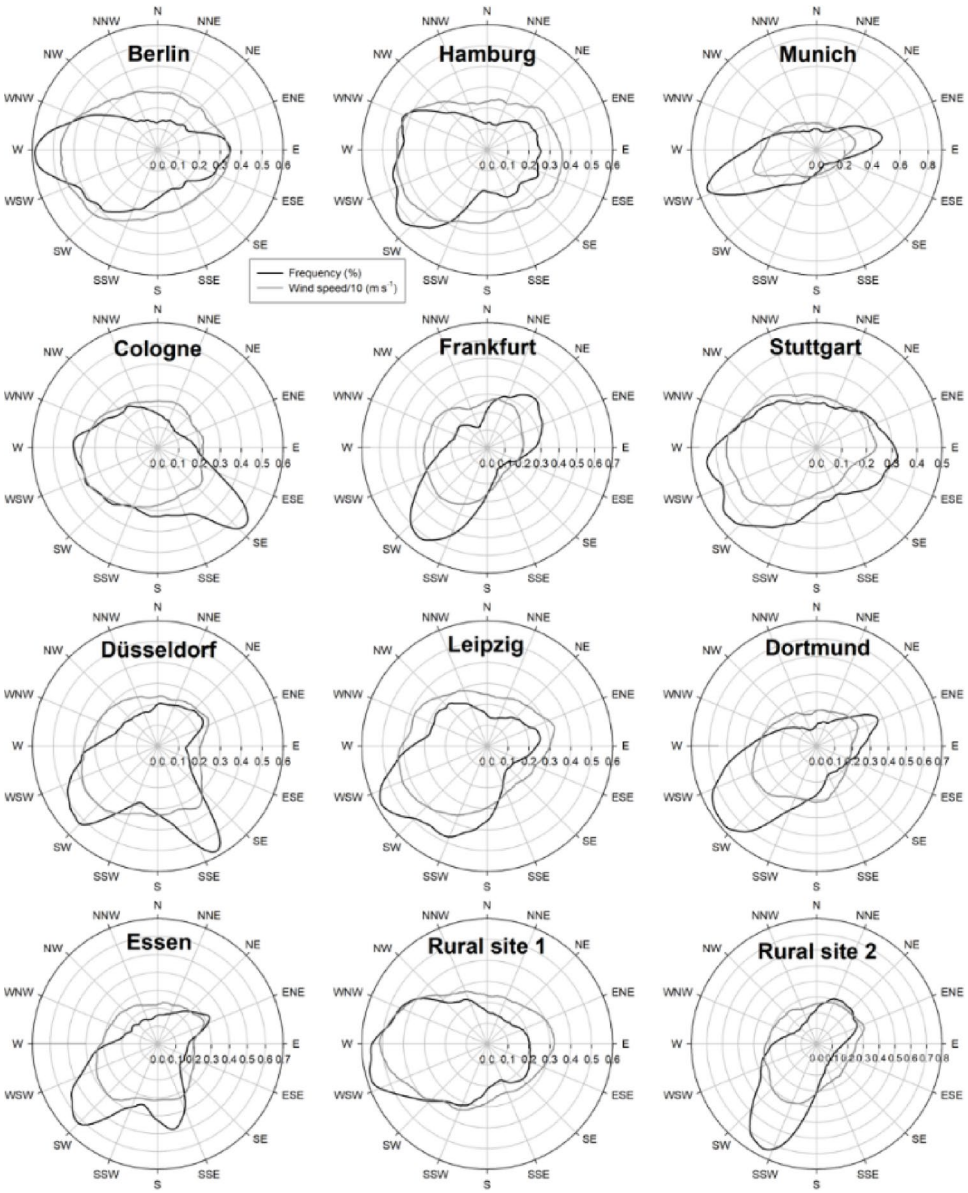

Fig. 3 - Wind direction and speed roses for the ten selected German cities and two rural sites

Wind roses with 8 and 16 sectors are presented in Figs. S1 and S2 for comparison. Worthy of note among them is the case of Essen, since the orographic influence attributed to the Rhine valley does not appear in both roses. In Dusseldorf, this influence only appears in the 16-sector rose. In any case, the definition of both the highest and lowest contributing directions is improved in the 1-degree roses presented in Fig. 3.

Wind speed values are quite steady since the lowest average for all the directions is observed in Stuttgart, 2.4 m s^{-1}, and the highest in Hamburg with 3.4 m s^{-1}, closely followed by Berlin. Moreover, the highest range was observed in Munich, which is noticeable for its low wind speed, 2.4 m s^{-1}. This result may be linked to the directional winds observed in this city. High wind speed values associated with frequent directions are observed in Berlin or Stuttgart, although the opposite case is possible, such as in Cologne, where the most frequent direction is not accompanied by high wind speed values and where the lowest range was observed, around 1.8 m s^{-1}.

Since wind direction roses determine specific sectors, their boundaries may be determined by the lowest values of frequencies. These are presented in Table 1 together with other noticeable magnitudes. The most relevant feature was the contrasting values of frequencies, which are around 30 or 60% in most of cases. Cologne and Frankfurt are the cities where this contrast is lower. On the other hand, the contrast between these two sectors is the highest in Leipzig or Rural site 1, around 50%. When three sectors are suggested, the sector which is explained by orographic reasons, i.e., the

Table 1 Frequencies of the wind direction sectors together with their associated wind speeds

City	Sector boundaries (degrees)	Frequency (%)	Average wind speed ($m\ s^{-1}$)
Berlin	161–358	64.25	3.74
	359 − 160	35.75	2.99
Hamburg	14–184	37.92	3.24
	185 − 13	62.08	3.59
Munich	16–152	33.20	2.12
	153 − 15	66.80	2.62
Cologne	47–205	46.92	2.44
	206 − 46	53.08	2.90
Frankfurt	152–338	57.43	3.12
	339 − 151	42.57	2.21
Stuttgart	18–156	34.50	1.97
	157 − 17	65.50	2.67
Düsseldorf	95–196	31.78	2.93
	197–346	46.09	3.34
	347 − 94	22.13	2.41
Leipzig	9-138	24.44	2.72
	139-8	75.56	3.35
Dortmund	154–345	65.09	3.02
	346 − 153	34.91	2.16
Essen	115–194	25.08	2.92
	195–344	48.13	3.16
	345 − 114	26.79	2.35
Rural site 1	38–161	24.63	2.82
	162 − 37	75.37	3.41
Rural site 2	122–311	62.73	3.19
	312 − 121	37.27	2.69

river valley, presents a frequency that is comparable to the rest of the sectors.

A multiple range test was conducted with wind speed data presented in Fig. 3, together with the sector classification. The contrasts are small for every city, with the highest differences being close to 1 $m\ s^{-1}$ for Düsseldorf and Frankfurt, whereas the lowest is observed in Hamburg, where it was about 0.4 $m\ s^{-1}$. However, all the differences are statistically significant at a 95% confidence level. This result reveals the agreement between wind sectors and their corresponding wind speeds.

3.2 Spatial Analysis by Wind Direction Sector

Figures S3-S14 present the direction turning for the ten selected cities and the two rural sites. Turning angles are small in Berlin and Hamburg. This result indicates that the influence of the city is weak.

Since comparing these representations may be not easy, the gradient was calculated in each grid node, and the average of the gradient magnitudes was obtained. This value may be compared with the magnitude of the average gradient. The magnitude of this average gradient will be small when isolines present rounded shapes, bands, or when the gradient is small. Figure 4 presents the result and may be analysed taking into account Fig. 2.

The highest values of the gradient magnitude averages were seen in certain sectors of Rural site 2 (ENE, E), Stuttgart (ESE and SE), and Frankfurt (ENE, E and ESE). In these latter cases, a marked city influence was observed since the values of the average gradient magnitude are small. Figure 5 presents a selection of specific cases. For instance, for Frankfurt with an E flow, a noticeable counter-clockwise turning was observed over the city with an intensive transition towards the NW of the region of around 60 degrees. However, isolines were located around some centres in Rural site 2, where cities are not considered. In order to establish the contrast between regions with or without a city the 95th and 90th percentiles of the gradient magnitude were calculated. This procedure was based on the high gradients observed in regions with cities. In this case of Rural site 2, these percentiles are lower than those for Frankfurt, which is the nearest city.

Moreover, under specific conditions, a marked change in direction was observed, although the city shape was not defined –for instance in Stuttgart with a S flow– which is also presented in Fig. 5. In this case clockwise turnings were observed in the south, and counter-clockwise turnings in the

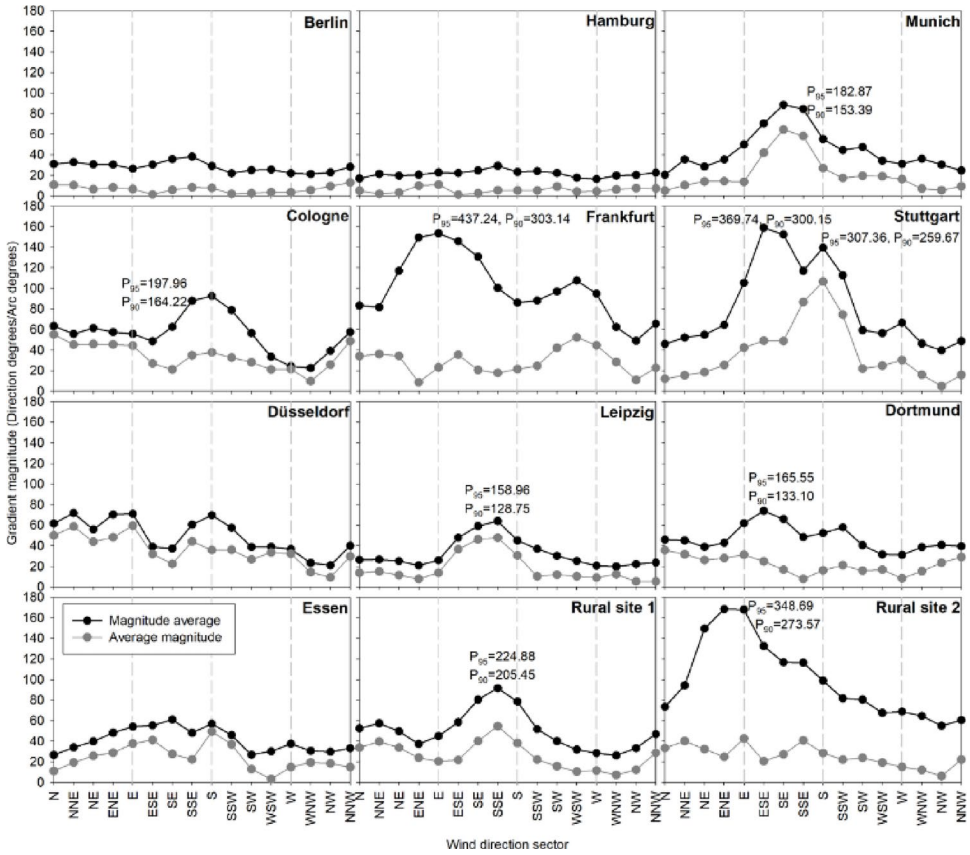

Fig. 4 - Comparison between the averages of gradient magnitudes (magnitude average) and the magnitude of the gradient average (average magnitude) for the ten selected cities and two rural sites following the 16 wind sectors. The 95th and 90th percentiles of selected gradient magnitudes are also presented

north. A displacement from the south to the north of the region implies a counter-clockwise turning with a similar value to that for Frankfurt in the previous case, although valley or slope induced flows might contribute to this result.

Similar behaviour –albeit with lower gradient values– was observed in other cities, such as Cologne (S). As Fig. 5 shows, direction turning (about 40 degrees) is smaller than for Frankfurt, although in this case it is noticeable. Moreover, the influence of this city can be seen in Düsseldorf. For their part, Munich (SE) or Leipzig (SSE) could be compared to Stuttgart (S). An isoline centre was observed in Rural site 1 for the SSE sector, Fig. S13. This could be attributed to the orographic influence of hills to the south. The lowest gradient values were obtained for Hamburg and Berlin.

Specific cases of Fig. 2b and c are observed in Essen (WSW) and Dortmund (W), respectively, both with very small gradients. These are also presented in Fig. 5.

Finally, Fig. 6 is based on the averages of gradient magnitudes presented as black dots in Fig. 4. Three groups may be observed. The first considers the biggest cities –Berlin and Hamburg –which have the smallest values of average and standard deviation from the 16 sectors, indicating that urban signals may depend on urban features such as urban roughness and urban extension. Most of the cities analysed fall into group 2, which presents intermediate values of the represented variables. Rural site 1 falls into this group. Finally, only two cities stand out for having the highest values –Frankfurt and Stuttgart– together with Rural site 2.

4 Discussion

The von Mises distribution is the extension of the Gaussian distribution to circular data (Benlakhdar et al. 2024). One noticeable drawback, however, is its single mode. Nevertheless, this disadvantage may be avoided by mixing some distributions. For instance, Nadarajah and Bell (2024) mixed some distributions to describe wind directions in South Africa. Although this extension appears simple, noticeable discrepancies with experimental values are observed if just a few distributions are used. Xu et al. (2025) obtained a better agreement with data at Yangshan Port, China, with an addition of six functions. This example reveals that the closed form of the wind direction distribution may be complex.

Smoothing procedures offer alternative ways of obtaining fast fits of directional data. Noise in experimental data may pose a handicap but can be avoided through suitable selection of the bandwidth (Diakhate et al. 2024; Zámečník et al. 2024). A suitable bandwidth should avoid rapid changes but should retain the contrast between the main contributing directions and the less frequent sectors. The current research used a kernel smoothing to calculate the direction

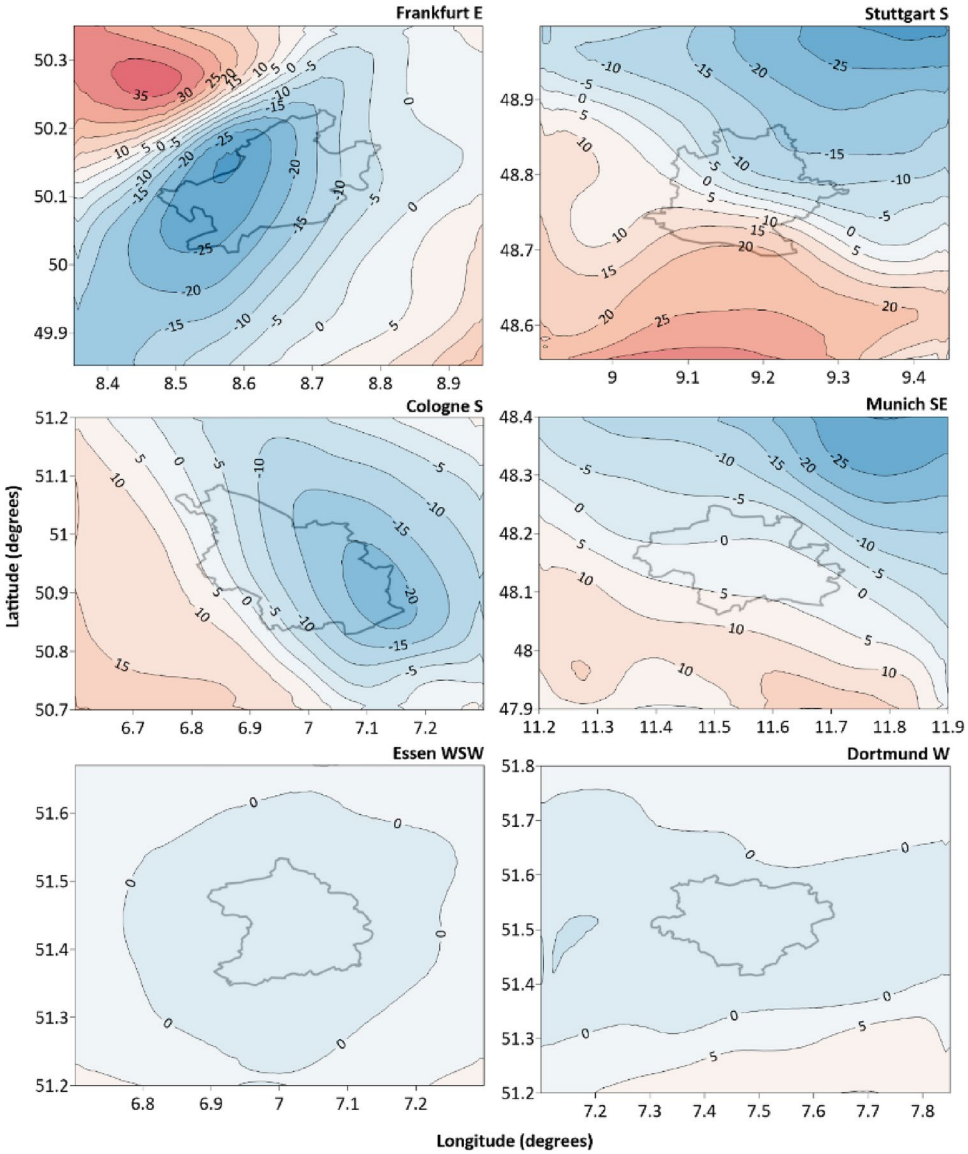

Fig. 5 - Wind direction turning (degrees against the average wind vector) for specific cases

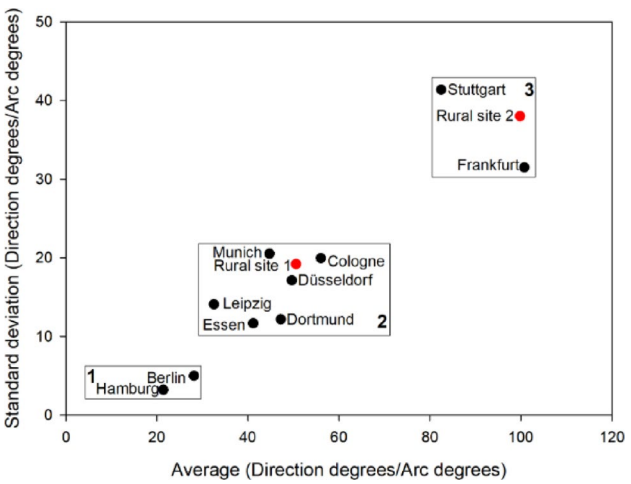

Fig. 6 - Averages and standard deviations calculated with the averages of gradient magnitudes presented as black dots in Fig. 4

roses although a method based on an iterative procedure was suggested for bandwidth determination. This is a fast procedure, which is determined by the data itself. Consequently, and in contrast to more theoretical procedures, this is an experimental procedure. The current study considers a fixed bandwidth for the whole distribution. However, Chau et al. (2025) recently suggested a variable bandwidth following the changes in data density. In their analysis with wind data from Binh Thuan, Vietnam, they suggested three bandwidth groups. Low bandwidths enhance details due to under-smoothing, which determines the loss of the general data structure. Medium bandwidths may trigger over-smoothing when data density is high, but under-smoothing when data density is low. Finally, large bandwidths may produce over-smoothing since detailed information about the data structure may be lost. Moreover, a second smoothing procedure based on a moving average was suggested in

the current research. This procedure is simpler than kernel smoothing, and its results were similar. This second procedure was presented for the wind speed rose.

Rose shape direction is determined by two types of factors. The first falls into the meteorology field, since the circulation pattern establishes the wind flow. The second factor is formed by the orographic features that condition this flow. Both factors were considered by Daniels et al. (2022) in their analysis of three sites at False Bay, South Africa.

The weight of these two factors depends on the case. Regional circulation patterns may play a key role in certain situations. For instance, Tošić et al. (2018) analysed the prevailing winds in Northern Serbia and indicated the following three pressure centres: the Mediterranean cyclone, the Siberian high, and the Azores anticyclone, although they also underlined the orography of the eastern Balkans. Chawla et al. (2018) investigated wind direction at the Rajec Ecosystem Station in the Czech Republic and concluded that the prevailing wind directions are not affected by the highland orography since they are determined by the general atmospheric circulation patterns over Europe. Moreover, seasonal evolution might modify the wind rose, and a more detailed analysis might prove necessary for practical purposes (Zhao 2025). Pan et al. (2024) presented the annual pattern of wind direction in Zhengzhou, China, with three prevailing sectors. However, the monsoon influence is noticeable in summer since a wide sector prevails against an opposite second sector with a small frequency.

The second factor affecting wind direction is topographic elements, which may have a noticeable influence on specific wind flows, such as the case presented by Lin et al. (2025), where a lee vortex was observed in Taiwan under NE flow. Lorente-Plazas et al. (2015) presented wind roses at different sites of the Iberian Peninsula, where contrasting results appear following orographic features. These included noticeable valleys to the northeast and south where prevailing directions are marked against the central plains where the circulation pattern determines the rose shape. Yu et al. (2025) presented the breeze effect at Hangzhou Bay, China, although the mountain wind's contribution to site cooling is stronger than the daytime sea breeze. Shang et al. (2024) analysed the sea breeze effect on the urban heat island in Tianjin, China. They suggested two 45-degree sectors perpendicular to the coastline as land and sea-breeze sectors and used two groups of meteorological stations to study this effect. One group is along the breeze direction, and the other group follows a perpendicular direction. The current paper underlines the usefulness of a detailed analysis of wind direction in a spatial network and investigates direction turning between the wind direction at every point of this network and the average wind direction. This contrasting city behaviour against wind direction could be explored, since building ventilation systems respond differently depending on wind direction (Almazmumi et al. 2025). He at al. (2025) presented an example with wind speed profiles in 16 sectors together with wind roses in Hong Kong, China. They selected the E-W and NE-SW directions where open spaces improve breezeway effectiveness.

Figure 3 reveals that the synoptic pattern determines the shape of these roses since the westerly component prevails against the easterly component. However, the specific shape, (such as the wide westerly sector for Hamburg) and orientation (such as the defined sectors for Munich or Frankfurt) could be affected by orography, with the Cologne rose being the most representative example. Moreover, these roses were obtained with the average wind for each region studied. This procedure avoids local patterns linked to specific sites, such as those presented by Seidler et al. (2024) where varied roses are obtained in the area surrounding Munich. In addition, the current study reveals the high frequencies of westerly winds for Stuttgart in Fig. 3, and Fig. S8 shows that this direction is steady since wind direction changes are small, except for the SSW sector where a counter-clockwise turning is observed in the city. Previous analyses for this city revealed the orographic influence since mountain breezes have been detected (Adler et al. 2020; Zeeman et al. 2022).

High resolution wind roses are not frequent. In this paper, calculations were made with a 1-degree resolution and were slightly smoothed to avoid some of the noise. With this resolution, specific wind sectors are well determined. Kirchner-Bossi and Porté-Agel (2018) presented 3-degree and 5-degree resolution roses for Horns Rev I and Princess Amalia –two offshore wind farms on the Dutch coast. The different appearance or shape was attributed to interpolation for a smooth contour against the direct values for a noisy shape (Feng and Shen 2015). Bulaevskaya et al. (2015) presented a 5-degree resolution wind rose at 90 m above ground level for a two-month campaign at Altamont Hills, California, where the prevailing wind direction pattern was very marked in a moderately complex landscape. Milla-Val et al. (2024) modelled wind speed over a complex terrain and presented a 10-degree resolution wind rose with two defined directions in the central region of the Pyrenees mountain range, Spain. Chen et al. (2025) presented the wind direction and speed roses for Qingdao, China, with a variable number of sectors ranging from four to 64 and concluded that this latter number of sectors generates the most accurate results since the distribution pattern is very defined. The current paper considers 1-degree resolution, which improves the definition of narrow contributing sectors, although it has the disadvantage of the noisy rose obtained. However, both iterative kernel smoothing or the mobile mean procedure avoid this inconvenience.

Wind roses suggest the prevailing directions, which may be used to plan urban corridors. Recent papers highlight their contribution for, among other benefits, reducing air pollutant concentrations, land surface temperatures (Fang and Zhao 2022), heatwaves and tropical nights (Son et al. 2022). Liu et al. (2025b) determined urban ventilation corridors for Shanghai, China in only two prevailing wind directions, although more directions were initially proposed. Liu et al. (2024) presented the city response for Nanjing, China, under wind patterns linked to the cooling and heating seasons and suggested ventilation corridors to highlight these effects. Wang et al. (2022) analysed Hangzhou, which is one of the hottest cities in China, and indicated that urban ventilation depends on green spaces, followed by water bodies and roads. Liu et al. (2022) suggested two corridors for Kaifeng, China, one in the east and the other in the west of the city. Both are parallel and follow the wind rose in the city. Similarly, Zhao (2025) analysed wind direction among other variables in the Nanhu District, Jianxing City, China, to determine urban ventilation corridors under the dominant wind direction.

These urban corridors may be considered as electric circuits where resistances indicate the ventilation resistance. This circuit theory was used in Wuhan, China, by Fang et al. (2023), who suggested a ventilation corridor model with a noticeable mitigation effect on the urban heat island under the prevailing wind direction against non-corridor areas. Similarly, 14 local ventilation zones were considered in Shenzhen, China, by Guo et al. (2025) and two types or corridors were suggested. These corridors –related with water bodies or green spaces– channel cool air to urban areas. However, some corridors may have a warming effect due to surfaces formed by asphalt and concrete. Moreover, some showed contrasting effects throughout the day or over the year.

Figure 5 reveals that the wind rose for the average wind in the region could not describe wind behaviour at a smaller scale, which perhaps suggests that finer-scale roses should be considered in order to obtain the correct wind path. In addition, wind direction presents a daily and annual evolution (Wang et al. 2025) and changes therein may be noticeable. For instance, Kong et al. (2023) studied the impact of a heatwave in 2020 on the urban heat island and on the wind field in the Greater Sydney Area, Australia. They considered three periods, with the first extending from January 23 to 29, which is the pre-heatwave. The second spans from January 30 to February 3, when the heatwave was observed. The third period, called the post-heatwave, lasted from February 4 to 10. Noticeable changes in wind direction were observed in some cases in this analysis, which spanned quite a limited period. The current paper avoids this problem, since the wind turning or direction departure against the mean direction was calculated for the spatial analysis. However, one disadvantage arises with extremely low wind speeds. Under these situations, all turning values are possible and turnings with opposite sign counteract. Moreover, the data extension is considerably large, and the results may be considered sufficiently robust since occasional outliers are masked by the general pattern.

The current research indicates that the response of the regions studied depends on the wind sector analysed; i.e. wind meandering is related to wind direction. However, in some direction sectors, wind direction changes are noticeable and reveal specific wind paths, which could be used in urban environments. Analyses that investigate urban response under different directions are not infrequent, albeit at a finer scale. Krawczyk et al. (2025) presented salient calculations about the urban influence on wind streamlines under different wind directions. Ma and Zhou (2025) modelled the response of wind flow in a street canyon, where a vortex is observed with the wind direction perpendicular to the canyon. A meandering flow is obtained under a wind direction of 45° with the street canyon and the flow is channelled when wind direction and canyon are parallel. Moreover, the vegetation response is considered since the flow is modelled in two cases; the first being for a centre single line tree planting and the second for two sideline tree-planting. Vortexes disappear when the wind direction is perpendicular and wind speed is smaller in the other two directions, i.e., for 45 and 0°. More complex examples were presented by Liu et al. (2025c). Detailed resolution is required to obtain information about the interaction between wind and buildings, such as in the analysis by Zhang et al. (2025b) where even the streamlines are represented.

Liang et al. (2023) underline the influence of urban surfaces on local wind patterns, with buildings determining vortexes and saddle points in their near-wake zone (Asami et al. 2021). The blockage produced by buildings was modelled by Hamze-Ziabari et al. (2024) for Lausanne, Switzerland, under two local dominant winds called Bise and Vent, coming from opposite directions, and they indicated the influence of wind channelling on the recorded measurements. This paper presents a marked contrast between the city and its surroundings due to the high resolution of this analysis. This contrast is not so clear in the current research, where the city boundaries are not experimentally observed, probably due to the 1-km resolution of the database. Reis et al. (2025) presented wind fields for one selected day in summer in Lisbon, Portugal, where estuarine breezes are the main mesoscale effect. The city effect is weak in early morning and late afternoon. However, the regular pattern of wind direction was seen to change at noon due to heat stress. Looking at the whole region presented, the role played by the city could be secondary, which concurs with the results

of the current research where the influence of the city is generally weak.

5 Conclusions

This paper presents a methodological framework for spatial wind direction analysis where hourly data over 18 years in ten German cities and two additional rural sites were used. Average wind direction is determined over selected regions as a specific feature of the current research. Smoothed rose calculation with 1-degree resolution avoids data noise and retains the main noticeable directions, with the bandwidth determination being a second original contribution. Three types of roses are observed. The reasons for the prevailing directions are the circulation pattern, which is the westerly in the cases studied, and orographic features, such as the SE direction in Cologne and Dortmund. The influence of topographic elements is not so clear in certain cities such as Stuttgart, probably due to the calculated spatial averages rather than roses for specific sites.

Direction turnings are suggested by this research and were calculated in the cities and their surrounding areas, and their responses depended on wind direction. Two turning patterns were observed. The first was represented by Frankfurt under an easterly flow, where turning centres were close and well defined. However, a second pattern formed by turning bands was observed –with Stuttgart under the south flow being the most representative example.

A procedure based on the contrast between two gradient calculations from the direction-turning field was suggested to determine the field shape. However, small differences were obtained in most of the cases considered, and the contrast between urban and rural sites is weak, probably due to the low resolution of the initial data. Berlin and Hamburg stood out for their weak response in this analysis.

Study limitations are closely related with further research, which could explore smoothing sensitivity against bandwidth or the implications of dispersion calculation of direction turnings. In addition, isolated flows, such as valley breezes, under specific circulation patterns may be a research objective, due to the detailed time resolution, which is sufficient to reveal the strength of the daily pattern. Moreover, annual and daily cycles could be explored to obtain more precise insights into how this variable evolves. Availability of a database with a higher spatial resolution would help to determine the wind corridor. Inclusion of techniques, such as machine learning or neural networks, or spatial analyses, such as geographic information systems or remote sensing, could provide deeper insights (Alif et al. in press; Alif et al. preprint; Alif 2025; Ghosh et al. 2025; Karamaj et al. 2026; Subramani et al. 2025). The current study reveals that this research field is open to new procedures that have practical applications in urban developments.

Supplementary Information The online version contains supplementary material available at https://doi.org/10.1007/s41748-026-01061-2.

Acknowledgements The authors acknowledge the Deutscher Wetterdienst for the database created by Stefan Krähenmann, Andreas Walter, Susanne Brienen, Florian Imbery, and Andreas Matzarakis.

Author Contributions Isidro A. Pérez: Conceptualization, Methodology, Software, Writing-Original Draft, Mª Ángeles García: Methodology, Investigation, Writing- Review & Editing, Orelvis Valdés: Writing- Review & Editing.

Funding Open access funding provided by FEDER European Funds and the Junta de Castilla y León under the Research and Innovation Strategy for Smart Specialization (RIS3) of Castilla y León 2021-2027. This research received no external funding.

Data Availability The dataset is available via doi:https://doi.org/10.5676/DWD_CDC/TRY_Basis_v001.

Declarations

Competing Interests The authors declare that they have no known competing financial interests or personal relationships that could have appeared to influence the work reported in this paper.

References

Adler B, Kalthoff N, Kiseleva O (2020) Detection of structures in the horizontal wind field over complex terrain using coplanar doppler lidar scans. Meteorol Z 29:467–481. https://doi.org/10.1127/METZ/2020/1031

Ali-Taleshi MS, Bakhtiari AR, Liu N, Hopke PK (2025) Characterization and transport pathways of high $PM_{2.5}$ pollution episodes during 2015–2021 in Tehran, Iran. Aerosol Air Qual Res 25:18. https://doi.org/10.1007/s44408-025-00016-y

Alif HA (2025) Temperature-based solar energy forecasting: a big data analysis for sustainable energy planning in Ishwardi and Rajshahi region of Bangladesh. Theor Appl Climatol 156:526. https://doi.org/10.1007/s00704-025-05746-y

Alif HA, Mashrafi MJ (preprint) Machine learning-driven rainfall forecasting model for sustainable and adaptive infrastructure planning (eds)

Alif HA, Mashrafi MJ, Elhag M, Purohit S (in press) Artificial intelligence-driven rainfall forecasting and GIS-based flood risk mapping for climate-resilient infrastructure in Bangladesh. Earth Syst Environ. https://doi.org/10.1007/s41748-025-00958-8

Almazmumi S, Sun H, Liu M, Calautit J, Jimenez-Bescos C (2025) A novel wall windcatcher (WWC) natural ventilation system evaluated through CFD and experimental field testing - a solution to single-sided ventilation in multi-story buildings? Build Environ 283:113307. https://doi.org/10.1016/j.buildenv.2025.113307

Asami M, Kimura A, Oka H (2021) Improvement of a diagnostic urban wind model for flow fields around a single rectangular obstacle in micrometeorology simulation. Fluids 6:254. https://doi.org/10.3390/fluids6070254

Ashrafi M, Chua LHC, Irvine KN, Yang P (2022) Spatiotemporal modeling of the wind field over an urban lake subject to wind sheltering. J Appl Meteorol Climatol 61:489–501. https://doi.org/10.1175/JAMC-D-21-0027.1

Benlakhdar S, Rziza M, Thami ROH (2024) In-depth analysis of von Mises distribution models: Theory, applications, and future directions. Stat Optim Inf Comput 12:1210–1230. https://doi.org/10.19139/soic-2310-5070-1919

Bing D, Zhaoyin Y, Wupeng D, Xiaoyi F, Yonghong L, Chen C, Yan L (2021) Cooling the city with natural wind: construction strategy of urban ventilation corridors in China. IOP Conf Ser: Earth Environ Sci 657:012009. https://doi.org/10.1088/1755-1315/657/1/012009

Brandi A, Martilli A, Salamanca F, Georgescu M (2024) Urban boundary-layer flows in complex terrain: dynamic interactions during a hot and dry summer season in Phoenix, Arizona. Q J R Meteorol Soc 150:3099–3116. https://doi.org/10.1002/qj.4752

Bulaevskaya V, Wharton S, Clifton A, Qualley G, Miller WO (2015) Wind power curve modeling in complex terrain using statistical models. J Renew Sustain Energy 7:013103. https://doi.org/10.1063/1.4904430

Chau T, Nguyen T, Nguyen L, Do T (2025) Wind speed probability distribution based on AdaptiveBandwidth Kernel Density Estimation model for wind farm application. Wind Energy 28:e2970. https://doi.org/10.1002/we.2970

Chawla S, Nguyen VX, Guerra Torres CP, Pavelka M, Trusina J, Marek MV (2018) Wind characteristics recorded at the Czech carbon observation system (CZECOS) site RAJEC. Eur J Environ Sci 8:117–123. https://doi.org/10.14712/23361964.2018.16

Chen X, Hu H, Xu Z, Wu Z, Ma R, Wang X (2025) Wind comfort criteria and numbers of wind directions: the dual impact mechanism on pedestrian wind comfort evaluation in Qingdao, China. Build Environ 280:113103. https://doi.org/10.1016/j.buildenv.2025.113103

Daniels T, Fearon G, Vilaplana A, Hewitson B, Rautenbach C (2022) On the importance of wind generated waves in embayments with complex orographic features – A South African case study. Appl Ocean Res 128:103355. https://doi.org/10.1016/j.apor.2022.103355

Diakhate B, Dhaker H, Ngom P (2024) The β-divergence for bandwidth selection in circular kernel density estimation. J Agri Biol Environ Stat 29:417–437. https://doi.org/10.1007/s13253-023-00572-z

Dou J, Sun J, Bornstein R, Miao S, Lu B, Wang J (2024) Downstream and upstream effects of urban chains on precipitation in Beijing. Atmos Res 308:107540. https://doi.org/10.1016/j.atmosres.2024.107540

Du S, Kuang X, Chen J, Shi X (2023) Identification and assessment of urban ventilation corridors in the urban canopy layer under dynamic wind directions. Building Simulation Conference Proceedings 18:2752–2759 https://doi.org/10.26868/25222708.2023.1543

Ebert C, Weiss J (2024) Flow reconstruction of urban wind fields for wind-based path planning. In: Dillmann A, Heller G, Krämer E, Wagner C, Weiss J (eds) New results in numerical and experimental fluid mechanics XIV. Springer Nature Switzerland AG, Cham, Switzerland, pp 519–528. DOI: https://doi.org/10.1007/978-3-031-40482-5_49

Fang Y, Zhao L (2022) Assessing the environmental benefits of urban ventilation corridors: A case study in Hefei, China. Build Environ 212:108810. https://doi.org/10.1016/j.buildenv.2022.108810

Fang Y, Zhao L, Dou B, Li Y, Wang S (2023) Circuit VRC: A circuit theory-based ventilation corridor model for mitigating the urban heat Islands. Build Environ 244:110786. https://doi.org/10.1016/j.buildenv.2023.110786

Feng J, Shen WZ (2015) Modelling wind for wind farm layout optimization using joint distribution of wind speed and wind direction. Energies 8:3075–3092. https://doi.org/10.3390/en8043075

Fisher NI (1993) Statistics analysis of circular data. Cambridge University Press, Cambridge

Garvey D, Bustillos M, Chang S, Cionco R, Creegan E, Scott Elliott D, Huynh G, Klipp C, Ligon D, Measure E, Quintis D, Torres M, Vaucher G, Vidal E Jr, Wang Y, Williamson C, Yarbrough J, Yee Y (2009) U.S. Army Research Laboratory Meteorological Measurements for Joint Urban 2003 (No.ARL-TR-4989)

Ghosh H, Rahat IS, Emon MMR, Mashrafi MJ, Al Arafat Tanzin MA, Mohanty SN, Kant S (2025) Advanced neural network architectures for tomato leaf disease diagnosis in precision agriculture. Discov Sustain 6:312. https://doi.org/10.1007/s43621-025-01149-1

Guo Q, Lin Y, Zhang X (2025) Identification and cooling effect analysis of urban ventilation corridors in coastal hilly cities: A case study of Shenzhen. Urban Clim 61:102393. https://doi.org/10.1016/j.uclim.2025.102393

Hamze-Ziabari SM, Jafari M, Huwald H, Lehning M (2024) Quantifying urban climate response to large-scale forcing modified by local boundary layer effects. Front Environ Sci 12:1438917. https://doi.org/10.3389/fenvs.2024.1438917

Han L, Zhao J, Zhang T, Zhang J (2022) Urban ventilation corridors exacerbate air pollution in central urban areas: evidence from a Chinese City. Sustain Cities Soc 87:104129. https://doi.org/10.1016/j.scs.2022.104129

He Y, Yin S, Lyu X, Zhang Y, Wong S, Tse TKT, Ng E (2025) Effectiveness of breezeway design strategies in urban redevelopment: adapting to varying future urban density and irregular street patterns. Build Environ 283:113326. https://doi.org/10.1016/j.buildenv.2025.113326

Hwang H, Lee J, Shin SA, You CR, Shin S, Park J, Lee JY (2024) Vertical profiles of $PM_{2.5}$ and O_3 measured using an unmanned aerial vehicle (UAV) and their relationships with synoptic- and local-scale air movements. Remote Sens 16:1581. https://doi.org/10.3390/rs16091581

Kamaraj P, Subramani D, Alif HA (2026) Agricultural impact on groundwater utilization in the Manimuktha sub-basin of Vellar River. Environ Earth Sci 85:16. https://doi.org/10.1007/s12665-025-12725-z

Ketterer C, Matzarakis A (2014) Human-biometeorological assessment of the urban heat island in a city with complex topography - The case of Stuttgart, Germany. Urban Clim 10:573–584. https://doi.org/10.1016/j.uclim.2014.01.003

Kirchner-Bossi N, Porté-Agel F (2018) Realistic wind farm layout optimization through genetic algorithms using a Gaussian wake model. Energies 11:3268. https://doi.org/10.3390/en11123268

Kong J, Zhao Y, Strebel D, Gao K, Carmeliet J, Lei C (2023) Understanding the impact of heatwave on urban heat in greater Sydney: Temporal surface energy budget change with land types. Sci Total Environ 903:166374. https://doi.org/10.1016/j.scitotenv.2023.166374

Krähenmann S, Walter A, Brienen S, Imbery F, Matzarakis A (2018) High-resolution grids of hourly meteorological variables for Germany. Theor Appl Climatol 131:899–926. https://doi.org/10.1007/s00704-016-2003-7

Krawczyk Z, Vuppala RKSS, Paul R, Kara K (2025) Urban wind field effects on the flight dynamics of fixed-wing drones. Drones 9:362. https://doi.org/10.3390/drones9050362

Li X, Lin K, Shu Y, Lin X (2023) Comparison of the influences of different ventilation corridor forms on the thermal environment in Wuhan City in summer. Sci Rep 13:13416. https://doi.org/10.1038/s41598-023-40211-8

Liang Q, Miao Y, Zhang G, Liu S (2023) Simulating microscale urban airflow and pollutant distributions based on computational fluid dynamics model: A review. Toxics 11:927. https://doi.org/10.3390/toxics11110927

Lin CY, Chen WM, Sheng YF, Chen WC, Cheung HC, Charles, Chou CK (2025) Exploration of complex physical and chemical processes of a severe haze episode over central Taiwan. Sci Total Environ 985:179729. https://doi.org/10.1016/j.scitotenv.2025.179729

Liu D, Zhou S, Wang L, Chi Q, Zhu M, Tang W, Zhao X, Xu S, Ye S, Lee J, Cui Y (2022) Research on the planning of an urban ventilation corridor based on the urban underlying surface taking Kaifeng City as an example. Land 11:206. https://doi.org/10.3390/land11020206

Liu J, She X, Wang J (2024) Comprehensive optimization of urban building cluster morphology based on microclimate: A two-level optimization approach. Sust Cities Soc 100:105005. https://doi.org/10.1016/j.scs.2023.105005

Liu K, Zeng Y, Qiu X, Zhong Y (2025a) Analysis of local water humidity effect characteristics based on meteorological data: A case study of Nanjing. Atmosphere 16:407. https://doi.org/10.3390/atmos16040407

Liu R, Wang Y, Zhang Y, Peng Z, Chen H, Li X, Li H, Li W (2025b) Analysis of the city-scale wind environment and detection of ventilation corridors in high-density metropolitan areas based on CFD method. Urban Clim 59:102274. https://doi.org/10.1016/j.uclim.2024.102274

Liu S, Zhu Z, Wu W, Zheng X, Zhang D, Peng D, Pang B (2025c) Effects of urban-like intersections and urban squares on pedestrian risk in a floodwater–wind joint environment. Sust Cities Soc 130:106560. https://doi.org/10.1016/j.scs.2025.106560

Lorente-Plazas R, Montávez JP, Jerez S, Gómez-Navarro JJ, Jiménez-Guerrero P, Jiménez PA (2015) A 49 year hindcast of surface winds over the Iberian Peninsula. Int J Climatol 35:3007–3023. https://doi.org/10.1002/joc.4189

Ma H, Zhou X (2025) Analysis of forced convective heat transfer at the facades of street canyon: effect of wind direction and tree planting. Energy Build 344:115918. https://doi.org/10.1016/j.enbuild.2025.115918

May M, Wald S, Suter I, Brunner D, Vardag SN (2024) Evaluation of the GRAMM/GRAL model for high-resolution wind fields in Heidelberg, Germany. Atmos Res 300:107207. https://doi.org/10.1016/j.atmosres.2023.107207

McQuillan KA, Allen GH, Fayne J, Gao H, Wang J (2025) Estimating wind direction and wind speed over lakes with surface water ocean topography and Sentinel-1 satellite observations. J Earth Space Sci 12:e2024EA003971. https://doi.org/10.1029/2024EA003971

Mikhailuta SV, Lezhenin AA, Pitt A, Taseiko OV (2017) Urban wind fields: phenomena in transformation. Urban Clim 19:122–140. https://doi.org/10.1016/j.uclim.2016.12.005

Milla-Val J, Montañés C, Fueyo N (2024) Economical microscale predictions of wind over complex terrain from mesoscale simulations using machine learning. Model Earth Syst Environ 10:1407–1421. https://doi.org/10.1007/s40808-023-01851-x

Nadarajah S, Bell W (2024) Spatial modeling of wind directions in South Africa. Earth Syst Environ 8:1477–1501. https://doi.org/10.1007/s41748-024-00400-5

Ng E, Yuan C, Chen L, Ren C, Fung JCH (2011) Improving the wind environment in high-density cities by Understanding urban morphology and surface roughness: A study in Hong Kong. Landsc Urban Plan 101:59–74. https://doi.org/10.1016/j.landurbplan.2011.01.004

Pan P, Li F, Zhu Y, Xu P, Shang Y, Liao R (2024) Identification of urban ventilation corridor system using meteorology and GIS technology: A case study in Zhengzhou, China. Atmosphere 15:1034. https://doi.org/10.3390/atmos15091034

Pardo-del Viejo L, Fernández-Rodríguez S (2025) 3D aerodynamic trajectories of aerobiological particles from biological sources under local-scale meteorological conditions using CFD. Aerobiologia 41:303–321. https://doi.org/10.1007/s10453-025-09853-1

Reis C, Oettl D, Lopes A, Nouri AS, Vasconcelos J (2025) Modeling the influence of summer sea and estuarine breezes on heat stress in Lisbon (Portugal) using GRAMM-SCI. Build Environ 272:112702. https://doi.org/10.1016/j.buildenv.2025.112702

Seidler J, Friedrich MN, Thomas CK, Nölscher AC (2024) Introducing the novel concept of cumulative concentration roses for studying the transport of ultrafine particles from an airport to adjacent residential areas. Atmos Chem Phys 24:137–153. https://doi.org/10.5194/acp-24-137-2024

Sen S, Roesler J (2020) Wind direction and cool surface strategies on microscale urban heat island. Urban Clim 31:100548. https://doi.org/10.1016/j.uclim.2019.100548

Shang M, Cao L, Guo J, Guo Z, Liu L, Zhong S (2024) Influence of pure sea breeze on urban heat island in Tianjin, China: A perspective from multiple meteorological observations. Atmos Res 304:107408. https://doi.org/10.1016/j.atmosres.2024.107408

Son JM, Eum JH, Kim S (2022) Wind corridor planning and management strategies using cold air characteristics: the application in Korean cities. Sust Cities Soc 77:103512. https://doi.org/10.1016/j.scs.2021.103512

Subramani D, Kamaraj P, Diriba D, Padder FA, Kuppanan DC, Alif HA (2025) A systematic GIS and remote sensing based approach for mapping groundwater recharge zones in Kallakurichi district, Tamil Nadu, India. Discov Sustain 6:1424. https://doi.org/10.1007/s43621-025-02253-y

Tošić I, Gavrilov MB, Marković SB, Ruman A, Putniković S (2018) Seasonal prevailing surface winds in Northern Serbia. Theor Appl Climatol 131:1273–1284. https://doi.org/10.1007/s00704-017-2044-6

Wang W, Wang D, Chen H, Wang B, Chen X (2022) Identifying urban ventilation corridors through quantitative analysis of ventilation potential and wind characteristics. Build Environ 214:108943. https://doi.org/10.1016/j.buildenv.2022.108943

Wang R, Gu Y, Liu Y (2025) A simple yet effective multivariate long sequence wind speed prediction model for urban blocks with spatio-temporal feature embedding. Energy 330:136725. https://doi.org/10.1016/j.energy.2025.136725

Wilks DS (2019) Statistical methods in the atmospheric sciences, fourth edition. Elsevier, Amsterdam

Xu F, Wu X, Zhang R (2025) Study of wind speed and direction at Yangshan Port. Renew Energy 247:122982. https://doi.org/10.1016/j.renene.2025.122982

Yin S, Zhang Y, Lin T, He Y, Liu T, Liao W, Zhan Q, Wong S, Lai W, Ng E, Xiao Y (2025) A fine-resolution ventilation performance spatial model at pedestrian-level based on wind tunnel studies for high-density neighborhoods. Build Environ 281:113207. https://doi.org/10.1016/j.buildenv.2025.113207

Yu B, Luo Z, Chen F, Xie P, Miao S, Zhong Y (2025) How complex terrains reshape urban wind patterns and cooling effects: evidence from a high-density weather observation network in Hangzhou

Bay, China. Sust Cities Soc 130:106526. https://doi.org/10.1016/j.scs.2025.106526

Zámečník S, Horová I, Katina S, Hasilová K (2024) An adaptive method for bandwidth selection in circular kernel density estimation. Comput Stat 39:1709–1728. https://doi.org/10.1007/s00180-023-01401-0

Zeeman M, Holst CC, Kossmann M, Leukauf D, Münkel C, Philipp A, Rinke R, Emeis S (2022) Urban atmospheric boundary-layer structure in complex topography: an empirical 3D case study for Stuttgart, Germany. Front Earth Sci 10:840112. https://doi.org/10.3389/feart.2022.840112

Zhan Q, Gao S, Xiao Y, Yang C, Wu Y, Fan Z, Wu J, Zhan M (2020) Impact mechanism and improvement strategy on urban ventilation, urban heat island and urban pollution island: A case study in Xiangyang, China. Int Rev Spat Plan Sustain Dev 8:68–86. https://doi.org/10.14246/irspsd.8.3_68

Zhang H, Lv L, Yao Z, Guo W, Wang X, Shan W, Li X, Shen X (2025a) Vertical variations of ozone transport flux at multiple altitudes and identification of major transport direction in the North China plain. J Environ Sci 155:488–500. https://doi.org/10.1016/j.jes.2024.05.046

Zhang Q, Li J, Lu H, Zou H, Li K, Liang Y, Yang B, Liu J (2025b) TH-MuSiC: A high-performance multi-scale NWP-LBM coupling framework with CPU–GPU architecture for high-fidelity real-time urban wind field simulation. Build Environ 283:113313. https://doi.org/10.1016/j.buildenv.2025.113313

Zhao C (2025) Intelligent extraction of urban ventilation corridors based on region growth algorithm with restricted direction. Sci Rep 15:16932. https://doi.org/10.1038/s41598-025-01804-7sss